IEEE Access
Multidisciplinary ⋮ Rapid Review ⋮ Open Access Journal

Received 14 February 2023, accepted 24 March 2023, date of publication 29 March 2023, date of current version 3 April 2023.

Digital Object Identifier 10.1109/ACCESS.2023.3263045

RESEARCH ARTICLE

Baseline Wander Removal Applied to Smooth Pursuit Eye Movements From Parkinsonian Patients

MEHDI BEJANI[1], ELISA LUQUE-BUZO[2], ARSEN BURLAKA-PETRASH[1], JORGE A. GÓMEZ-GARCÍA[1], JULIÁN D. ARIAS-LONDOÑO[1], (Senior Member, IEEE), F. GRANDAS-PÉREZ[2], JESUS GRAJAL[1], (Senior Member, IEEE), AND JUAN IGNACIO GODINO-LLORENTE[1], (Senior Member, IEEE)

[1]ETSI Telecomunicación, Universidad Politécnica de Madrid, 28040 Madrid, Spain
[2]Movement Disorders Unit, Neurology Department, Hospital General Universitario Gregorio Marañón, 28007 Madrid, Spain

Corresponding author: Juan Ignacio Godino-Llorente (ignacio.godino@upm.es)

This work was supported by the Ministry of Economy and Competitiveness of Spain under Grant DPI2017-83405-R1 and Grant PID2021-128469OB-I00. All authors contributed in the same manner.

This work involved human subjects or animals in its research. Approval of all ethical and experimental procedures and protocols was granted by the Ethics Committee of Hospital de Fuenlabrada and Hospital Gregorio Marañón.

ABSTRACT Prior studies aiming to parametrize the sequences obtained from the Smooth Pursuit Eye Movements (SPEM) of patients with Parkinson's disease are based on the manual extraction of cues of interest. This is because methods to automatically extract the relevant information are complex to implement and are constrained, in part, by the appearance of a baseline wander (BW). Thus, new methods are required for preprocessing the SPEM sequences to make the potential parameterisation procedures much more robust, removing the aforementioned BW. In this respect, the present study compares different BW removal methods applied to SPEM sequences based on several objective evaluation metrics. At the same time, it proposes a set of guidelines to estimate the ground truth that is required for comparison purposes. Data were collected using a high-speed video-based eye-tracking device. 52 patients and 60 controls and 12 young participants were enrolled in the study. The ground truth required to compare the different BW removal techniques was manually delineated according to a predefined protocol. Seven methods were developed to remove the BW, and four objective metrics were used to evaluate the results. According to the results, a method based on the Empirical Wavelet Transform provided the best performance removing the BW. Furthermore, the objective and subjective results show that potential asymmetries between left and right eye movements are solved by removing the BW. Regardless of the techniques used, BW removal is revealed to be a crucial step for any autonomous SPEM processing tool.

INDEX TERMS Eye movements, smooth pursuit, baseline wander removal, Parkinson's disease.

I. INTRODUCTION

Parkinson's disease (PD) is a neurodegenerative disease that is due to the death of dopaminergic neurons in the substantia nigra. This degeneration leads to the classic motor symptoms of the disease, such as bradykinesia, tremors at rest and rigidity [1]. In addition, certain nonmotor symptoms are present in these patients, including eye movement defects. Oculomotor abnormalities are present not only in PD but also in some other neurodegenerative movement disorders, such

The associate editor coordinating the review of this manuscript and approving it for publication was Gyorgy Eigner.

as multiple system atrophy and Huntington's disease. These abnormalities are documented in at least 75% of patients with PD [2], [3], [4].

In PD patients, abnormal findings on clinical examination of eye movements are subtle, such as mild hypometria of voluntary saccades; and evident abnormalities raise suspicion of other parkinsonisms [10]. This is why laboratory recordings of eye movements are emerging as an objective and accurate assessment of the abnormalities related to the disease.

Seven types of eye movements are typically identified: fixation, saccades, smooth pursuit, optokinetic reflex, vestibulo-ocular reflex, nystagmus, and vergence [5]. However, most studies concentrate on the analysis of three eye movements: fixation, saccades, and smooth pursuits [6], [7]: *fixations* are tiny involuntary displacements that seek to stabilise and keep the focus on a fixed point of interest; *saccades* are rapid eye movements that abruptly redirect the gaze from one point of interest to another; *smooth pursuit eye movements* (SPEM) are used to keep the image of a moving object in the fovea. Despite the interest in fixations and saccades for the analysis of PD, this paper is devoted to the study of SPEM.

SPEM tests were designed to evaluate in real time the ability of a subject to follow the exact path of a moving target object [8]. When this is not the case, corrective movements are elicited in the form of saccades to catch up to the moving target. While the presence of saccadic movements during SPEM is considered normal, their frequency, extent, and type are different in patients with PD compared to normal subjects [9]. Several types of abnormal and involuntary saccadic movements have been reported in the literature [9], namely *corrective saccades*, which are elicited to eliminate existing delays when SPEM lags with respect to a moving target; *anticipatory saccades*, a type of ballistic movements that anticipate future target positions; and *saccadic intrusions*, which are involuntary movements taking the form of an initial fast movement away from the expected eye position followed by a return secondary saccade or a drift. The presence of these corrective movements leads to a detectable decrease in saccade amplitude and increased saccade latency, as well as a slightly impaired smooth pursuit with catch-up saccades [10]. PD patients also report reduced SPEM speed and gain, compared to the normal population.

SPEM analysis is of clinical interest in evaluating PD individuals, as shown by the proliferation of different studies and approaches on this topic [6]. Unlike other types of eye movements, SPEM are based on tracking targets in motion and are dependent on motion perception in the middle temporal area of the brain. Reciprocally, this area of the brain is essential for the generation of SPEM [11]. This dependence emphasises the relationship between the oculomotor and perceptual structures. Consequently, SPEM has been identified as helpful in the determination of disorders such as PD, due to its correlation with motor dysfunctions [11], [12].

Reference [6] presents a complete systematic review of the abnormalities found in SPEM of PD patients. However, despite the clinical interest in this technique, there are still gaps to be filled before translating the SPEM analysis into the clinical practise. This is because their analysis is far from being simply due to artifacts imbricated in the sequences gathered.

SPEM sequences are mainly captured using techniques based on either electro-oculography (EOG) or video-oculography (VOG). EOG records the electrical activity (corneo-retinal standing potential) generated between the front and the back of the human eye, through a set of electrodes placed in the lower and upper eyelids [13]. Unlike EOG, VOG involves cameras and image processing algorithms to determine the horizontal and vertical positions of the eye, either analysing the reflexions on the cornea or determining the pupil position. EOG is computationally less expensive; however, VOG offers a more convenient, more accurate, and less invasive method of measuring eye movements [14], which makes it more appropriate for clinical settings. Due to the nature of SPEM, the sequences obtained from these tests merge information on voluntary and involuntary eye movements. Involuntary movements are mainly of saccadic origin (i.e., saccadic intrusions, corrective saccades, and anticipatory saccades), whereas the voluntary movement in SPEM corresponds to a low frequency sinusoidal pattern of the eyes while following the target. This voluntary movement introduces a Baseline Wander (BW) in the SPEM sequences, which is also contaminated with other sources of information. The BW might be considered an artifact causing the amplitude of the SPEM sequence to drift up or down, obscuring the potential analysis of the involuntary movements. For EOG based SPEM sequences, the BW includes voluntary movements of the eyes and other undesirable effects related to electrode-based capture methods. In contrast, in VOG, the BW is yet induced by voluntary movements of the eyes, but also contains information from other sources: calibration issues, ambient noise in the environment, undesired vision disorders, troublesome head movements, certain attentional problems, and any software or recording equipment issues. In either case, the BW could tumble down a potential automatic analysis of SPEM recordings, since BW perturbations can mask the involuntary movements, which are of specific interest and are typically a subject of investigation.

As will be discussed later, removal of BW in EOG signals —as well as in other electrode-based recording methods— has been extensively addressed in the literature. However, to the best of the authors' knowledge, no previous work has dealt with the problem of BW removal in SPEM sequences recorded with VOG equipment. In this context, we pose the idea of removing the BW from the SPEM VOG-based (VOG-SPEM) sequences as a required step for the further analysis of saccadic movements, which are the primary source of information for evaluating different neurodegenerative diseases (including PD). We hypothesise that this preprocessing/denoising step would be of interest to isolate the involuntary movements of the eyes and for a potential

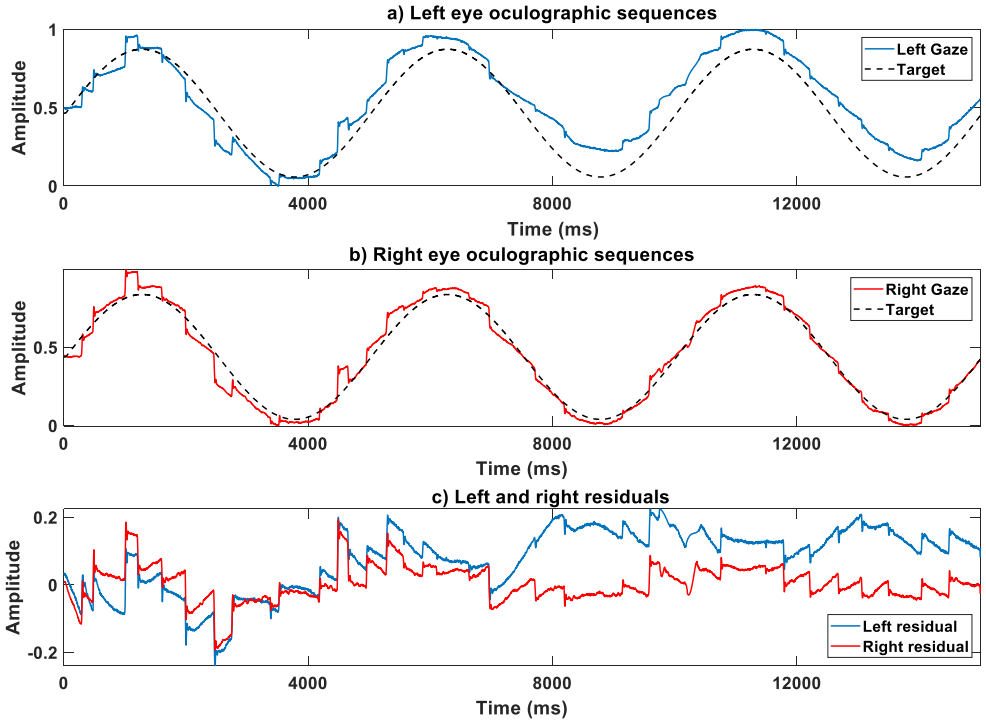

FIGURE 1. Illustration of VOG-SPEM sequences corresponding to the patient HF011. a) target and gaze positions for the left eye; b) target and gaze positions for the right eye; c) residual obtained by subtracting the sinusoidal background from the left and right eyes positions.

automatic parameterisation and analysis of the VOG-SPEM sequences using signal processing and artificial intelligence techniques.

Another fact supporting the need for BW removal procedures is the necessity to remove the apparent asymmetries that usually appear between both eyes in VOG-SPEM. These apparent asymmetries are unreal since both eyes are supposed to move synchronously and symmetrically [15], [16]. Such coordination is explained because, in binocular vision, the visual system combines the resulting, somewhat varied retinal images, to generate a single percept, which triggers a sensorimotor process that requires eye movements to keep the lines of sight of the left and right eyes pointing to the same target. In this respect, each eye has six muscles that control movement in different directions. The brain also uses a feedback system to precisely adjust the strength of the 12 muscles for each intended gaze direction. But, calibration problems, head movements of the subject during recording, certain attentional problems, and vision disorders (e.g., nearsightedness) lightly deviate the VOG-SPEM sequences from the target, suggesting a potential lack of coordination and/or symmetry, which, in fact, might not be present.

To illustrate this phenomenon in VOG-SPEM, Fig. 1 shows the target and gaze positions of a) the left eye and b) the right eye (both corresponding to participant HF011). Fig. 1c shows the sequences corresponding to the residual gaze position for the left and right eyes obtained by removing the gaze's sinusoidal background (target position). Although different events appear at the same instant in time, the existing BW might suggest certain asymmetries in the movement of both eyes.

A potential solution to eye asynchrony is to develop techniques for removing BW. BW removal is a well-known task in biomedical signal processing contexts. In the past, this problem has been reported and analysed for other bioelectrical signals such as EOG [17], [18], electromyogram (EMG) [19], [20], electrocardiogram (ECG) [21], photoplethysmographic signals [22], and pulse signals [23], among others. In these cases, BW occurs primarily due to improper placement of the subject's electrodes, changes in skin resistance, or electrode polarization, but other unavoidable events could also cause it, such as the participant's respiration and perspiration (causing electrode impedance modifications). Although of a different nature, these unpreventable events are also found in video-oculography, which is of interest in their proper detection and removal, since if not addressed, they would drift the estimated subject's absolute point of gaze [18].

The literature reports several techniques for the removal of BWs, with a particular focus on ECG applications. Most of these methods are generally based on infinite impulse response (IIR) or finite impulse response (FIR) high-pass filters, adaptive filtering, and moving average filters; or based on the decomposition of the signals by using methods such as empirical mode decomposition (EMD), variational mode decomposition (VMD), and empirical wavelet transform (EWT). In addition, different metrics were used

to evaluate the estimated BW: metrics based on distance (absolute maximum distance, sum of squares of the distances, percentage root mean square difference.-PRD), and statistics-based metrics (mean square error, cross-correlation, signal noise ratio.-SNR). A traditional approach to remove BW in ECG is to use a high-pass filter with a cutoff frequency of 0.7 Hz [24]. In [25] the authors compare different IIR filters (Butterworth, Elliptic, Chebyshev I, and Chebyshev II) to remove the BW from the ECG sequences, and used SNR as a metric [25]. Additionally, bandpass, adaptive, and Kalman filters were used in [26] and [27] implements a non-linear filter bank to remove BW in ECG signals. When the undesirable effects to be removed include nonlinear and nonstationary changes (transients and fundamental frequency variations), data-driven techniques, which can adapt to the characteristics of the data, are more commonly used than filter-based approaches. Most of these techniques are based on decomposing the signal into different time and frequency scales that provide tools for extracting low- and high-frequency information; also, they can perform locally and auto-adaptively [28]. These techniques include the discrete wavelet transform (DWT), EMD, EWT, and VMD [28], [29], [30], [31], [32], [33]. In this sense, [34] compared methods based on Kalman filtering, moving average filtering, cubic splines, DWT, and EMD, suggesting the use of an approach based on EMD as the best method to remove the BW. In [35], the authors compared different mother wavelets using MSE and SNR metrics for the removal of the BW, and the Sym10 wavelet yielded the best result for their data set. In [31], a hybrid approach of EMD, discrete wavelet transforms, and constrained least squares was used for BW denoising. A similar approach is discussed in [28], using VMD instead of EMD. In [36], EWT, was used for BW removal from ECG signals, showing better performance compared to standard linear filters and EMD.

In parallel to ECG applications, the literature also reports the removal of BW for other biomedical signals. In [37], the authors used a technique based on the quadratic variation reduction method to remove BW from ECG, EMG and electroencephalographic (EEG) signals. In [38], the authors used a linear deconvolution technique to correct the BW of the EEG signals. Furthermore, several approaches have been proposed to remove the BW from the EMG signals [19], [20], [39]. Likewise, pulse signals are also affected by BW, and its removal is the first preprocessing step to correctly measure diagnostic parameters [40]. In [41], the authors remove the BW of pulse signals using a method based on an energy ratio and a Meyer wavelet filter. Similarly to other biomedical signals, EMD was used to remove BW and reconstruct clean pulse signals [23].

Furthermore, previous works have also highlighted the need for BW removal in EOG [42], [43], [44]. In [17] and [18], different methods were used to remove the BW from EOG signals recorded for human-computer interaction applications. The techniques included signal differencing, high-pass filters, frequent resetting, and multilevel wavelet decompositions. The authors concluded that frequent resetting and signal differencing best remove the BW drift; however, frequent resetting is impractical as it disrupts the user's interaction, whereas signal differencing alters the morphology of the EOG signal, so they finally opted for a high-pass filter which showed a similar performance than the wavelet transform with less complexity. This result is in line with those presented in previous works [45], [46] where high or median pass filters and wavelet transforms were used, independently or in combination, for a similar purpose. Since EOG is an electrode-based acquisition method, the nature of the perturbations to be removed differs from those of VOG. Thus, these methods cannot be straightly extrapolated.

On the other hand, despite the extensive literature in the field, the problem of removing the BW in VOG-SPEM sequences poses certain challenges because of significant difficulties in the estimation of the ground truth (GT) to be used for comparison purposes. Thus, one of the main challenges of this work is the definition of a protocol to manually delineate the GT that will be used for further comparison.

The main objective of this work is to propose and compare different automatic methods for removing the BW from VOG-SPEM sequences. As commented, this preprocessing step is crucial to separate the voluntary and involuntary movements of the eyes, to allow a simple evaluation of the synchronisation and coordination of the left and right eyes, and for potential automatic processing of these sequences using machine learning techniques. As commented, this process requires the definition of a set of guidelines to estimate the GT that will be used for comparison purposes. These are important milestones to be reached to transfer the SPEM analysis to clinical practise. In this respect, this work contributes to the translational medicine [47] in videoculography by proposing solutions to BW removal in SPEM sequences.

The paper is organised as follows. Section II presents the materials and methods to record the data set and clinical assessments. Section III describes the criteria and protocols for the delineation of the BW, the metrics to evaluate the estimated BW, and the methods to remove the BW. Section IV shows the results of the experimental analysis and discussion. The conclusions are finally drawn in Section V.

II. MATERIALS

A. PARTICIPANTS AND CLINICAL ASSESSMENTS

52 patients with PD and 48 healthy subjects of the same age and sex were recruited as controls (Ctrl). Additionally, for comparison purposes and to understand the relationship between age and PD, 12 young controls (Yng) were recruited. The mean age of the PD patients was 63.8 years (range 44–84 years), 64.26 years for the Ctrl group (range 46–80 years), and 25.04 years (range 23–30 years) for the Yng cohort. Eleven out of the recorded participants' eye movements were discarded due to critical failures during the recording process (double corneal reflexes, participants' inability to follow the target, etc.). Furthermore, one of the PD

patients was diagnosed with MSA during clinical assessments and was also discarded from the analysis. Therefore, 41 PD, 47 Ctrl and 12 Yng participants were available for analysis.

The oculographic data of all participants were recorded over a period of two years at two university hospitals of the Madrid Community, Spain: the Fuenlabrada Hospital and the Gregorio Marañón Hospital.

All participants received a clinical evaluation and their medical history was recorded, including details such as the age of onset of PD, duration of the disease, symptoms, and complications. Patients with PD were assessed using the Movement Disorder Society - Unified Parkinson's Disease Rating Scale (MDS-UPDRS) part III, the Montreal Cognitive Assessment (MoCA), and the Beck Depression Inventory. The mean of UPDRS for PD was 16.88 and for Ctrl was 1.5.

This study was approved by the Ethics Committee of the Fuenlabrada and Gregorio Marañón Hospitals. All study participants received written informed consent and signed for participation.

B. RECORDING AND TASKS

Eye movements were recorded with an infrared video-based binocular EyeLink©1000 Plus (SR Research Ltd, Ontario, Canada) sampling at 1 kHz. The process is driven by two computers: one to control the eye-tracking system and another to present the stimuli. A LED monitor, which is attached to the second computer, was placed 60 cm in front of the patient.

The participant was seated with the head resting on a chin rest. The distance from the upper knob of the camera to the front of the chin rest is 50 cm. Before each recording session, the eye tracker system was calibrated using a 9-point grid that covers the area in which the targets were presented.

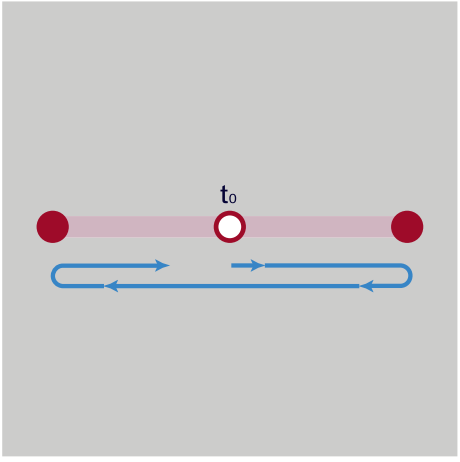

FIGURE 2. Illustration of the stimulus presented to the participants. Participants fixate on a small white dot for 200 ms. which was placed in the centre of the screen. After that, the white point disappears, and a red moving dot appears in the centre of the screen. The SPT follows the pattern of the red dot following the horizontal component of a pendulum-like movement. The red-point stimulus moves according to the arrow directions in the figure.

Participants were required to fix their gaze on a small white dot in the centre of the screen for 200 ms (Fig. 2). Then a red dot moving target immediately appears on the screen. The Smooth Pursuit Task (SPT) was performed following the pattern described in Fig. 2. The SPT follows the pattern of the red dot that moves with a certain frequency (0.2 Hz) and amplitude (6 degrees) following the horizontal component of a pendulum-like movement. The maximum viewing angle is chosen to avoid potential head movements during the test.

III. METHODS AND METRICS

A MATLAB® custom software was developed to perform different processes: data import, preprocessing, blink removal, and analysis of the sequences extracted from the VOG device.

During blinks, the eyelid closure creates a sudden artifact in the sequence, making the amplitude go towards infinite, which is followed by a subsequent sudden decrease towards the initial (or slightly similar) position after the eyelid opening. Meanwhile, the complete closure of the eyelids reports no position of the eyes. Thus, blinks are preceded and followed by these high amplitude artifacts, which make difficult an automatic interpolation process of the sequence. Blinks are initially detected using the automatic tools provided by the EyeLink 1000 Plus device. However, the boundaries identified require a manual review process to identify the beginning and end of these sudden increases and decreases of amplitude, not to include them in the subsequent interpolation process. The time interval between the beginning of the increase in amplitude and the end of the decrease was removed, and the middle segment was interpolated by using the Piecewise Cubic Hermite Interpolating Polynomial (PCHIP) method [48].

To establish comparisons, as stated above, a GT is required to compare different techniques of BW removal. Therefore, the GT was manually delineated using the criteria and protocols described below. The process is carried out in two stages: first, the initial estimate of the BW was performed using a simple moving average filter; subsequently, two experts manually manipulated and adjusted the initially estimated sequence to obtain the final sequence that will be used as GT for comparison purposes.

A. CRITERIA FOR MANUAL BW DELINEATION

The simplified objective of manual delineation is to obtain the GT that will be used for comparison purposes. The GT should follow the path the participant follows with the gaze, assuming that there are no involuntary movements. Ideally, the GT should be a sinusoidal pattern similar to the target movement. However, most of the VOG-SPEM recordings present a gaze that is shifted with respect to the target in the presence of certain events (e.g., saccadic intrusions, blinks, etc). These gaze shifts alter the baseline. Moreover, the gaze points are also shifted with respect to the target because of drifts that occur due to calibration problems or due to compensation for the lag with the target. Therefore, a protocol is required

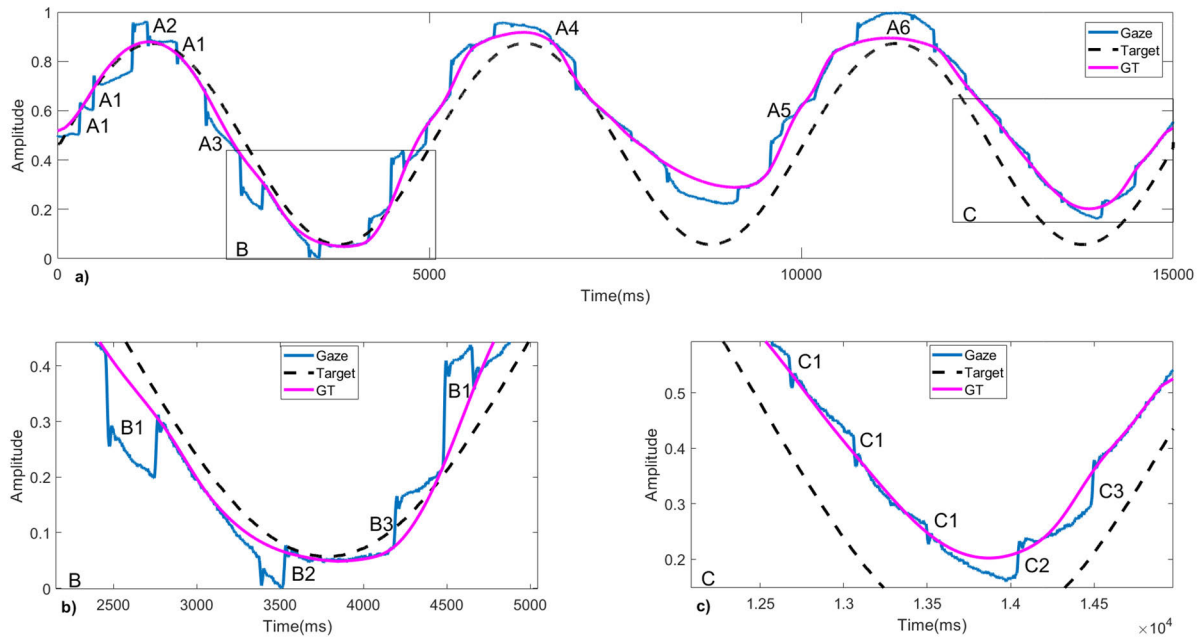

FIGURE 3. Example of SPT performed by participant HF011 (left eye, showing only horizontal movements). Figure 3a shows the following events: compensatory saccades during the latency period in which the participant adapts to the target velocity (A1), a corrective saccade solving an anticipatory saccade caused by the participant not expecting the deacceleration of the target (A2), noncorrected anticipative saccade at the steady region (A3) and at a maximum region (A4); an interpolated blink (A5) and a corrective saccade solving an anticipative saccade (A6) followed by a slight drift. Figure 3b shows saccadic intrusions composed of an anticipative saccade followed by an intersaccadic interval and a corrective saccade (B1), a corrective saccade reaching the target after a drift (B2), and a noncorrected anticipative saccade (B3). Figure 3c illustrates saccadic pursuit composed of compensatory saccades (C1), corrective saccade after a drift (C2), and a saccade that defines a new pathway for the gaze (C3).

to correctly delineate the GT at each of the events/scenarios that might be identified in the video-oculographic recordings. According to the type of event addressed, this protocol is divided into three sections: procedures to follow for saccadic events, for saccadic pursuit, and for eyes drifting.

1) SACCADIC EVENTS

The protocol defines different procedures to follow for each saccadic event that is present. Each of them is presented next:

a) Saccadic intrusion **with intersaccadic interval**: the GT curve would go through the starting point of the first saccade (in most cases an anticipative saccade) and it passes through the middle of the second saccade (could be back-up or corrective). This is due to the backup saccade normally not stopping at the target and going beyond it, therefore requiring a third smaller saccade that corrects the backup/corrective saccade. The end of this third saccade was the point chosen for the GT pathway, as shown in Fig. 3b for saccadic intrusions in B1.

b) Saccadic intrusion **without intersaccadic interval**: the GT will go through the starting point of the saccadic event, and it will pass through the end of the saccade, leaving the whole event outside the baseline.

c) Anticipative saccades followed by fixation or drift: the end of the fixation is the pathway to choose, as shown in the event A3 of Fig. 3a.

d) Noncorrected anticipative saccade: in case of an anticipative saccade starting a new pathway for the gaze that differs from the expected one, the baseline will go through the initial point of the saccade (unless a drift is present previously, which is the case for the event C3 in Fig. 3c) and will converge with the gaze.

e) Corrective or compensatory saccades: the baseline curve would be restrained by the end of the saccade as it would be the result of the correction of a previous event. Consecutive corrective saccades could be identified as compensatory saccades for an insufficient VOG-SPEM gain, which are common during the latency period (see A1 in Fig. 3a), but if they were present in most part of the signal, it would imply a saccadic pursuit (see C1 in Fig. 3c).

2) SACCADIC PURSUIT

In case the VOG-SPEM sequence suggests a saccadic pursuit behaviour, the baseline curve is delimited by the end of the consecutive compensatory saccades, allowing the proper isolation of the saccadic pursuit defining events and characteristics (low VOG-SPEM gain that coerces several compensatory saccades). The residual would show the well-known cogwheel pattern. Simplifying, this baseline would define the pathway that the participant is trying to follow but is not able to, requiring multiple saccadic movements to compensate for the low VOG-SPEM gain (see Fig. 3c).

3) EYE DRIFTING

The eyes sometimes show inertial behaviour at the points in which the stimulus changes direction (corresponding to the **extreme points** of the target sequence). Thus, the gaze is displaced, going beyond the stimulus, and increasing the amplitude of the VOG-SPEM sequence. The following scenarios were considered for these cases:

a) **With corrective saccade:** there are cases in which a corrective saccade is performed to reach the target again, the end point of this saccade being the reference point to draw the GT through the event (see A2 in Fig. 3a).
b) **With an anticipative saccade:** a drift from the target could be preceded by an anticipative saccade that is not corrected by a backup saccade, rather than slowly correcting the movement until reaching again the target after the amplitude of the extreme points. In these cases, the GT is drawn taking the starting point of the saccade as a reference to continue until the gaze reaches the target again (or at least close to it as in the event A6 in Fig. 3a).
c) **With two corrective saccades:** in some cases, normally in the first maximum of the first period of the sequence (influenced by the latency period), the drift could be corrected by two consecutive corrective saccades separated by an intersaccadic interval. It could be considered that both saccades are part of the same event of correction or that they are two independent saccades. The first approach was chosen and, therefore, when this event appears, the GT was established considering the end of the second corrective saccade.
d) **No saccade:** there are scenarios in which no saccades occur. In this case, the GT is drafted considering the target sequence, moving it one-third of the maximum amplitude of the gaze drift. This decision was taken to properly isolate the drift of the eye from the target as an event to be considered.

In addition to the aforementioned scenarios, sometimes a saccadic intrusion appears at the extreme points in which the stimulus changes its direction. This scenario could be identified as either a correction of the drift or as an independent event. These cases require a specific evaluation of the participant's gaze behaviour with respect to the target. Generally, the drift appears as a product of the inability of the participant to decelerate at the same rate as the target. Therefore, the drift event and its corresponding corrective saccade (in case it exists) would be below the target line at a minimum and above the target at a maximum. If this occurs, accepting this event as a corrective saccade is considered correct, so the already described procedure is applied (this is the criterion applied for case A6 in Fig. 3a). If not, the possibility of this event being a saccadic intrusion should be considered.

The appearance of a drift or displacement is also possible (but not as common) in the steady regions in which the velocity is constant, therefore not being directly caused by the deceleration of the stimulus. These cases could be explained by participant distraction and, normally, are solved by a corrective saccade, with the GT drafted following the same criteria as in the extreme points.

B. METRICS FOR EVALUATING THE SIMILARITY OF TWO SEQUENCES

Four similarity metrics were used to quantitatively evaluate the similarity of the estimated BW with respect to the manually delineated GT.

To prevent possible signal strength (amplitude) bias, the sequence was first normalised, ensuring that all sequences are within the same range.

The four metrics used are explained below assuming two sequences, $s_1[m]$ and $s_2[m]$, with a length of R samples, where $s_1[m]$ is the GT sequence, $s_2[m]$ is the estimated sequence, and m is the number of the current sample of the sequence.

1) Percentage Root-Mean-Square Difference Metric (PRD) (eq. 1): PRD is a widely used similarity metric based on distance (1). It ranges in the interval [0, 100], with 0 being the best value.

$$\mathrm{PRD}\,(s_1[m],s_2[m]) = \sqrt{\frac{\sum_{m=1}^{R}(s_1[m]-s_2[m])^2}{\sum_{m=1}^{R}(s_1[m]-\bar{s_1})^2}}100\% \quad (1)$$

where $\bar{s_1}$ is the mean value of the original sequence, $s_1[m]$.

2) Root Mean Squared Error (RMSE) (eq. 2): it is the square root of the mean square of all the errors (2). RMSE ranges in the interval [0.. ∞), being 0 the best value.

$$\mathrm{RMSE}\,(s_1[m],s_2[m]) = \sqrt{\frac{\sum_{m=1}^{R}(s_2[m]-s_1[m])^2}{R}} \quad (2)$$

3) Symmetric Mean Absolute Percentage Error (SMAPE) (eq. 3): measures the accuracy of an estimation system as a percentage according to (3),. SMAPE provides values in the interval [0, 200], with 0 being the best value.

$$\mathrm{SMAPE}\,(s_1[m],s_2[m]) = \frac{1}{R}\sum_{m=1}^{R}\frac{|s_2[m]-s_1[m]|}{(|s_2[m]|+|s_1[m]|)/2}100\% \quad (3)$$

4) Signal Noise Ratio (SNR) (eq. 4): compares the GT level with the level of the residual. The residual is the difference between the GT and the estimated sequence. SNR is defined as the ratio of GT power to residual power (4). SNR provides values in the interval [0.. ∞), being ∞ the best value.

$$\mathrm{SNR}\,(s_1[\,m],\,s_2[\,m]) = 20\cdot\log_{10}\frac{\sqrt{\sum_{m=1}^{R}s_1[\,m]^2}}{\sqrt{\sum_{m=1}^{R}(s_1[\,m]-s_2[\,m])^2}} \quad (4)$$

The goal is to get the smallest feasible value for PRD, RMSE and SMAPE and the largest values for SNR; thus, the estimated BW is regarded as the closest approximation to the GT.

TABLE 1. Mean value and std. of the objective metrics used for the seven BW removal methods developed. Results aggregated (all), for Ctrl, PD, and Yng groups.

Method		PRD	RMSE	SMAPE	SNR
EMD	PD	15.90 ± 17.32	0.044 ± 0.040	9.98 ± 5.27	24.77 ± 5.67
	Ctrl	18.47 ± 15.76	0.051 ± 0.037	10.79 ± 5.45	23.65 ± 6.34
	Yng	7.55 ± 3.55	0.025 ± 0.011	8.68 ± 3.17	28.47 ± 3.67
	All groups	15.95 ± 14.94	0.045 ± 0.034	9.64 ± 4.42	24.49 ± 5.61
VMD	PD	13.54 ± 15.06	0.038 ± 0.036	8.30 ± 4.54	26.21 ± 5.68
	Ctrl	14.76 ± 12.40	0.040 ± 0.028	8.50 ± 4.11	25.37 ± 5.93
	Yng	6.10 ± 2.62	0.020 ± 0.008	7.51 ± 2.73	30.18 ± 3.36
	All groups	13.22 ± 13.12	0.037 ± 0.031	8.30 ± 4.15	26.29 ± 5.76
FDM	PD	12.33 ± 13.25	0.035 ± 0.031	9.78 ± 5.02	26.67 ± 5.16
	Ctrl	12.74 ± 10.06	0.035 ± 0.023	10.49 ± 4.94	26.07 ± 4.99
	Yng	6.14 ± 1.94	0.020 ± 0.006	9.68 ± 3.81	29.81 ± 2.45
	All groups	11.78 ± 11.12	0.033 ± 0.026	10.10 ± 4.85	27.19 ± 5.97
EWT	PD	**10.80 ± 12.87**	**0.030 ± 0.030**	8.69 ± 4.80	**28.28 ± 5.52**
	Ctrl	**10.65 ± 8.99**	**0.029 ± 0.021**	9.14 ± 5.21	**27.92 ± 5.38**
	Yng	**4.92 ± 1.37**	**0.016 ± 0.004**	9.19 ± 4.22	**31.68 ± 2.34**
	All groups	**10.02 ± 10.44**	**0.028 ± 0.024**	8.96 ± 4.92	**28.52 ± 5.28**
MAF	PD	11.73 ± 13.93	0.033 ± 0.033	**6.98 ± 4.39**	27.72 ± 5.83
	Ctrl	12.57 ± 11.18	0.034 ± 0.026	**7.38 ± 4.12**	27.11 ± 6.40
	Yng	5.21 ± 2.03	0.017 ± 0.006	**6.45 ± 2.83**	31.45 ± 3.16
	All groups	11.34 ± 11.96	0.032 ± 0.028	**7.10 ± 4.10**	27.88 ± 6.00
IIR	PD	11.34 ± 12.43	0.032 ± 0.030	8.54 ± 5.11	27.70 ± 5.75
	Ctrl	11.78 ± 9.88	0.033 ± 0.024	9.05 ± 4.95	27.20 ± 5.74
	Yng	5.21 ± 2.22	0.017 ± 0.007	8.08 ± 3.56	31.51 ± 3.27
	All groups	10.81 ± 10.65	0.030 ± 0.026	8.72 ± 4.86	27.92 ± 5.65
EMD2	PD	11.40 ± 12.00	0.032 ± 0.030	8.86 ± 5.88	27.56 ± 5.72
	Ctrl	11.46 ± 9.08	0.032 ± 0.023	9.15 ± 5.17	27.16 ± 5.46
	Yng	5.30 ± 2.06	0.017 ± 0.006	8.14 ± 3.30	31.24 ± 2.94
	All groups	10.78 ± 10.22	0.031 ± 0.025	8.95 ± 5.30	28.00 ± 5.45

C. METHODS EVALUATED FOR REMOVING THE BW

This section presents a brief description of the techniques evaluated to remove the BW of the VOG-SPEM sequences, $s_2[m]$.

Five of them are based on decomposition techniques, which are common methods used to identify modal information in time-domain signals. In this work, following the indications in [49] and [50], different modes were extracted and combined in the search for the best estimate of the BW. Since BW is a low-frequency artifact, it is expected that the main BW components will be located in the low-frequency modes (i.e. the last ones, according to the usual criterion of decomposition) of each of the methods used. For comparison purposes, two additional techniques based on IIR and moving average filters were also implemented. The methods evaluated are the following[1]:

1) Empirical mode decomposition (EMD): EMD was first introduced in [51]. It is a method for decomposing a time domain signal into several sub-bands using an iterative approach. These various components (corresponding to the sub-bands) are termed intrinsic mode functions (IMFs). Since EMD is entirely data-driven, there is no need to decide how many IMFs to use. The signal is decomposed using the EMD method from high to low frequency, with the lowest frequency component remaining in the residual. IMFs do not have a predefined frequency range, since the number of IMFs may vary depending on the signal. Therefore, to distinguish between clean and noisy IMFs for BW estimation, human intervention is usually required. In this work, the estimated BW of the VOG-SPEM was calculated by aggregating the last six IMFs and the residual. This parameter (six) was obtained by iteratively aggregating the IMFs (from last to first) until the best estimate was obtained. (Figure 9a in Appendix 2).
2) Variational mode decomposition (VMD): initially proposed in [52]. Like EMD, VMD is a sequential process that decomposes a signal into different IMFs that reconstruct the original signal jointly. The primary distinction is that the VMD approach uses a non-recursive but analytical decomposition technique where the IMFs are decomposed simultaneously around their centre frequency, whereas EMD decomposes the signal adaptively and is data driven. To select clean IMFs, new

[1]The source code of the methods is available at: https://github.com/BYO-UPM/BW-SP-Analysis-PD This repository also contains several SPEM examples, their associated manually delineated ground truth, and a simple interface to display the results.

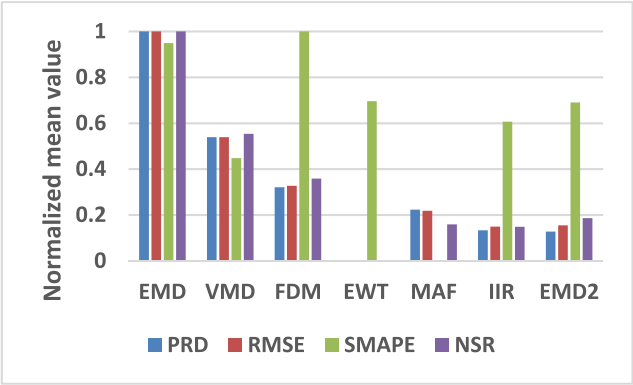

FIGURE 4. Normalized mean value (based on the maximum and minimum values) for each method and metrics of SPT sequences (for the SNR metric, the graphic shows NSR=−SNR for coherence with the other metrics). The missing values are equal to 0 (0 corresponds to the minimum of the normalized value, and 1 to the maximum).

experiments are required because the VMD is a completely different approach from the EMD. The optimum BW of VOG-SPEM was obtained using only the last extracted IMF (Fig. 9b in Appendix 2).

3) Fourier Decomposition Method (FDM): the FDM, first introduced in [53], is an adaptive signal decomposition method based on the well-established discrete Fourier transform and the use of zero-phase non-causal FIR filters. The method is efficient for the analysis of nonlinear and nonstationary time series. This study used a high-pass filter with a 0.6 Hz cutoff frequency for the FDM method (Fig. 9c in Appendix 2).
4) Empirical Wavelet Transform (EWT): EWT is also a method for decomposing a time series into various modes. Although the EMD presents an excessive number of modes, the EWT provides a more consistent decomposition. Unlike EMD, which lacks a mathematical foundation, EWT is a fully adaptable, data-driven signal processing technique with a well-defined mathematical background. The Fast Fourier Transform of the signal is computed initially, followed by the calculation of the boundaries using the segmentation of the Fourier spectrum, and finally the acquisition of various modes using an adaptive wavelet filter bank based on the boundaries [54]. In this work, the VOG-SPEM sequences are decomposed into three modes through EWT, and the last three modes are selected to estimate BW. The best number and combination of modes are obtained by testing different scenarios (Fig. 9d in Appendix 2).
5) Moving Average Filter (MAF): this method was used in [55] to eliminate BW in ECG signals. It gives local k-point means, where each mean is computed for k-point sliding windows of nearby elements in the sequence. The method behaves like a low-pass filter computed in the time domain. In this study, the value of k was experimentally fixed at 600 (Fig. 9e in Appendix 2).
6) IRR filtering: an IIR high-pass filter with a cutoff frequency of 0.5 Hz was used. The cutoff frequency was experimentally identified by testing different values (Fig. 9f in Appendix 2).
7) EMD2 (EMD by high-pass filtering each IMF): this method is based on a combination of an EMD and an IIR filtering. In this work, the VOG-SPEM sequences were first decomposed into the number of IMFs identified by the EMD method and then filtered with an IIR filter which was applied to the last six IMFs. The estimated BW of the VOG-SPEM is extracted by summing up the last six filtered IMFs and the residual. In this work, a high pass filter with a 0.9 Hz cut-off frequency was used (the cut-off frequency is experimentally obtained by testing different values (Fig. 9g in Appendix 2).

Appendix 2 details the different experiments that were carried out to identify the best hyperparameters of each method. Note that differences in the cutoff frequencies are expected for the different methods, as reported in [56].

IV. RESULTS AND DISCUSSION

Table 1 shows the mean value of the metrics used for each method and the Ctrl, PD, and Yng cohorts. As can be seen in this table, the Yng group has low values for PRD, RMSE, and SMAPE metrics and high SNR values. Furthermore, individually, for the three cohorts (Ctrl, PD, and Yng), and according to the PRD, RMSE and SNR metrics, the best BW removal method is the one based on EWT, although MAF provided competitive results according to the SMAPE metric.

However, the differences in metrics between the Yng and Ctrl groups and the Yng and PD groups reported significance (Table 2 in the appendix). However, there are no significant differences in the metrics obtained between the PD and Ctrl cohorts (Table 2 in the appendix). This is attributed to the fact that participants in the Yng group could easily follow the target; thus, the estimated BW using the different methods contains small differences concerning the GT. At the same time, in the Ctrl and PD cohorts, patients report more difficulties following the target, which are corrected with saccadic events, producing certain divergences between the estimated BW and the GT.

Table 1 shows the mean value for each method and the metrics of the SPT sequences for the aggregation of all cohorts. As shown in Table 1 and Fig. 4, the EWT performs better than the remaining methods based on PRD, RMSE, and SNR metrics; but for SMAPE, MAF performs better than other methods.

Beyond the error results and the selection of the best method according to the GT, it is also important to analyse the limit cases in which the removal methods, and particularly EWT as the best method so far, do not perform as expected. Fig. 5 shows those cases with the worst performance of BW removal. These examples are presented to highlight the errors committed in BW removal using EWT. Fig. 5a shows the results for participant HG051 (right eye), which has a high value of RMSE and a low value of SNR (RMSE = 0.143 and SNR = 12.51 for the EWT method). Fig. 5b shows the results

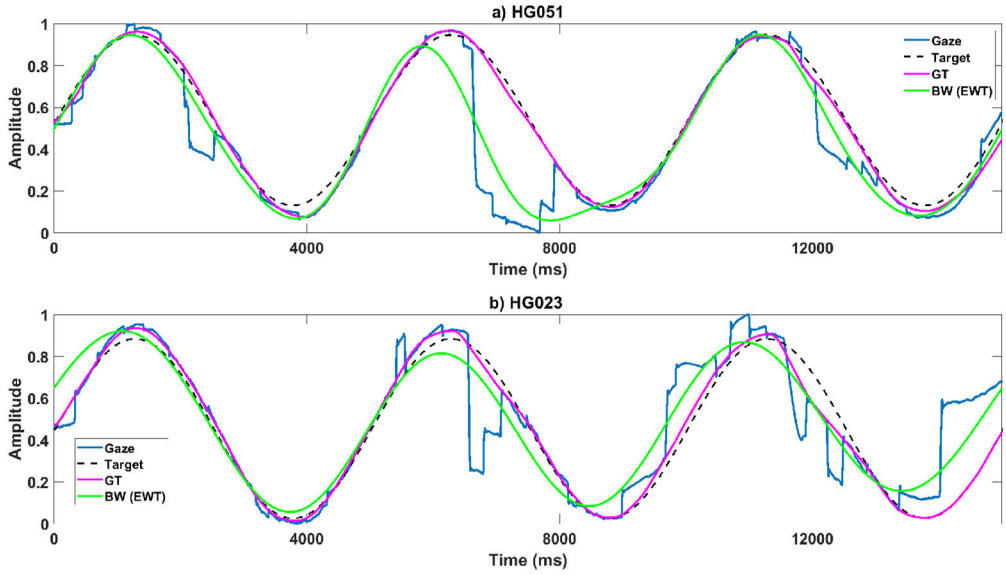

FIGURE 5. Results using the EWT method for those participants reporting the worst metrics: a) HG051 (PD patient with H&Y = 2).; b) HG023 (Ctrl participant who was very nervous during the recording session, and required multiple repetitions).

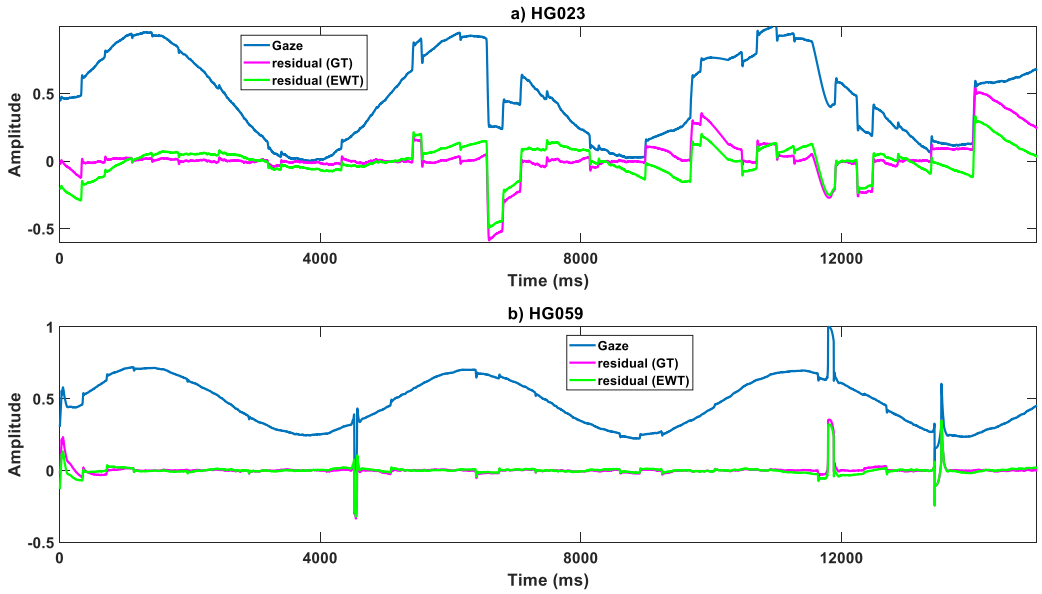

FIGURE 6. The residual sequence for: a) the case with the worst performance of the BW estimation using EWT (HG023); b) the case with the best performance of the BW estimation using EWT corresponds to a rigid-akinetic PD patient with H&Y=1 (HG059).

for the participant HG023 (left eye), which has a high value of PRD and SMAPE (PRD = 47.68 and SMAPE = 31.8 for the EWT method). The bias between the estimated BW and the GT is due to the presence of different strong involuntary events in the sequences.

Furthermore, the inaccuracies in the BW estimation observed in Fig. 5 might leave unwanted artifacts in the obtained residual sequences after BW removal. Fig. 6 shows two examples of residual sequences calculated by removing the BW (estimated using EWT) from the gaze position. Fig. 6a shows the residual sequence for the participant who reported the worst results (HG023). As expected, this Fig. shows that the residual best revealing all involuntary events is obtained by removing the GT from the gaze position. However, the residual obtained by subtracting the estimated BW also shows such involuntary events. In contrast, Fig. 6b shows the participant who reported the best results (HG059). The alignment between the residual sequence obtained by

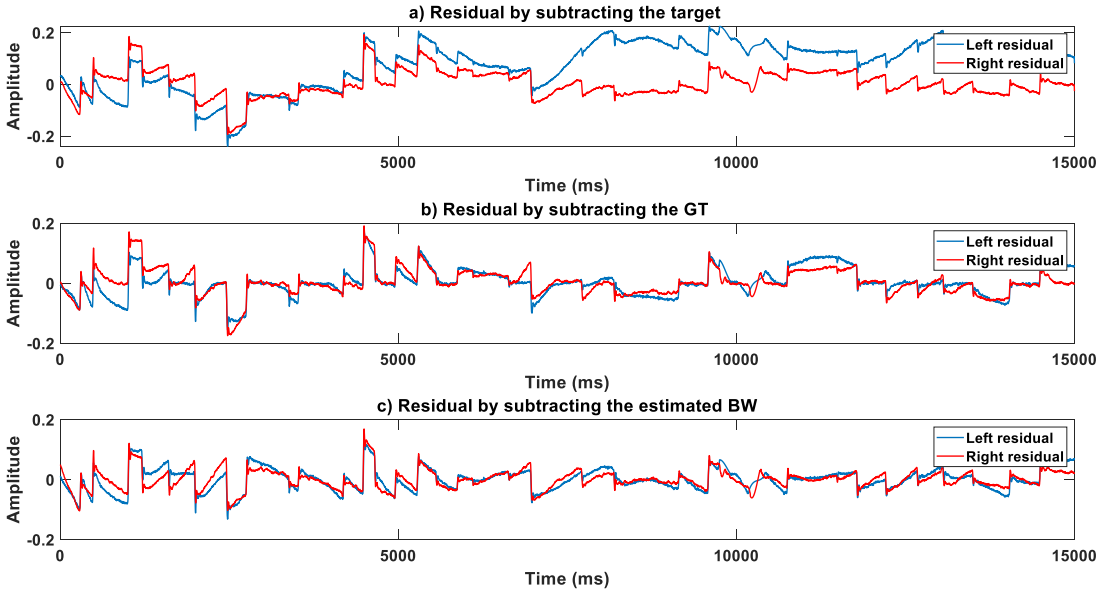

FIGURE 7. Illustration of the residual for the patient HF011: a) residual calculated by subtracting the sinusoidal background from the left and right eyes positions; b) residual obtained by subtracting the manually delineated GT from the positions of the left and right eyes; c) residual calculated by subtracting the BW (by EWT) from the positions of the left and right eyes.

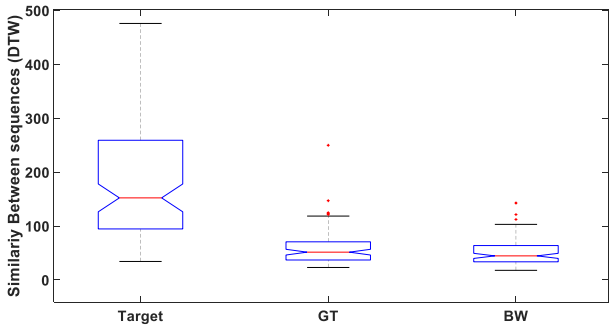

FIGURE 8. Box plot of the DTW similarity metric between left and right residuals subtracted from the Target (i.e. sinusoidal pattern), GT, and BW (by EWT). For the sake of comparison, 8 outliers were removed from the target column.

removing the BW (estimated using EWT) and that obtained by removing the GT is excellent.

Notwithstanding, in certain limit cases, some spurious behaviours persist. The recovered alignment of VOG-SPEM observed in Fig. 6b after removal of BW is in line with the expected synchronisation between the eyes. In this sense, Fig. 7a shows the existing asymmetries between the two eyes reported in Fig. 1, which are due to calibration and recording issues. Furthermore, Fig. 7b displays the residual signal obtained by subtracting the GT from the gaze position of the participant HF011, and Fig. 7c shows the residual obtained by subtracting the estimated BW (by EWT) from the gaze position of the participant HF011. Figs. 7b and 7c show that the expected symmetry is recovered after the BW removal. The asymmetries between the two eyes for the residual signal obtained by subtracting the target (i.e. sinusoidal pattern), GT, and BW (using EWT) from the gaze position were evaluated for all subjects in the experiments using a similarity metric based on dynamic time warping (DTW) [57], reporting 242.39 (std. 347), 59.52 (std. 32), and 50.71 (std. 22) for the three types of residuals, respectively. Fig. 8 shows the box plots of the DTW similarity metric obtained. The results suggest that the removal of the BW solved the asymmetries between the two eyes. However, after removing the BW, there are still certain asymmetries, since individuals with PD and elder Ctrl may be lightly impaired in binocular coordination during SPEM [12], [58].

V. CONCLUSION

VOG-SPEM sequences merge voluntary and involuntary eye movements. The voluntary movements correspond to a quasi-stationary low frequency sinusoidal-like sequence with a main component centred on the frequency of the stimulus, whereas involuntary movements are mainly of saccadic origin and contain high-frequency components. This voluntary movement introduces a BW in the VOG-SPEM sequences, which is considered an artifact causing the amplitude of the VOG-SPEM sequence to drift up or down. The BW also contains information from other sources, including calibration issues, environmental noise, attentional problems, vision disorders, head movements, and potential software or recording equipment problems. Therefore, we propose the idea of removing the BW for a further analysis concentrated on the involuntary movements alone, which are the main source of information for the evaluation of different neurodegenerative diseases (including PD). Additionally, accurate removal of BW is considered a crucial step for a clinical evaluation of the synchronisation and symmetries in the movements of both eyes.

TABLE 2. The p-values of the differences between the metrics obtained for the three groups.

Method	Groups	PRD	RMSE	SMAPE	SNR
EMD	PD vs. Ctrl	0.30	0.28	0.31	0.22
	PD vs. Yng	0.02	0.02	0.25	0.003
	Ctrl vs. Yng	0.001	p<0.001	0.07	p<0.001
VMD	PD vs. Ctrl	0.57	0.62	0.70	0.38
	PD vs. Yng	0.02	0.02	0.44	0.002
	Ctrl vs. Yng	0.001	p<0.001	0.26	p<0.001
FDM	PD vs. Ctrl	0.82	0.89	0.34	0.44
	PD vs. Yng	0.02	0.02	0.93	0.005
	Ctrl vs. Yng	0.002	0.002	0.45	p<0.001
EWT	PD vs. Ctrl	0.92	0.85	0.39	0.57
	PD vs. Yng	0.03	0.02	0.38	0.004
	Ctrl vs. Yng	0.002	0.002	0.80	p<0.001
MAF	PD vs. Ctrl	0.66	0.72	0.53	0.51
	PD vs. Yng	0.02	0.02	0.58	0.003
	Ctrl vs. Yng	0.002	0.002	0.30	0.002
IIR	PD vs. Ctrl	0.80	0.90	0.50	0.56
	PD vs. Yng	0.02	0.02	0.68	0.002
	Ctrl vs. Yng	0.002	0.002	0.37	p<0.001
EMD2	PD vs. Ctrl	0.80	0.90	0.50	0.56
	PD vs. Yng	0.02	0.02	0.68	0.002
	Ctrl vs. Yng	0.002	0.002	0.37	p<0.001

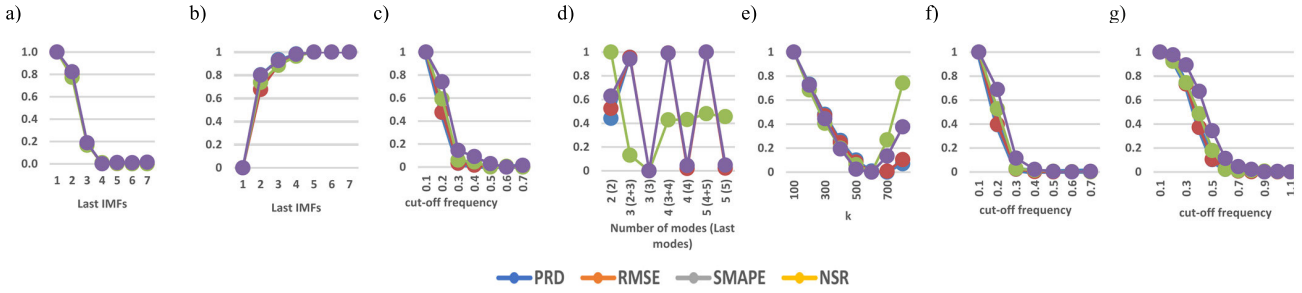

FIGURE 9. Influence of the hyperparameters of each method in the results (normalized amplitude). a) Performance of the EMD method for different accumulated number of IMFs; b) Performance of the VMD method for different accumulated number of IMFs; c) Performance of the FDM method vs. cut-off frequency; d) Performance of the EWT method vs. maximum number of modes and combination of modes required to estimate the BW; e) Performance of the MAF method vs. k values; f) Performance of the IIR method vs. cut-off frequency; g) Performance of the EMD2 method for different cut-off frequencies of the residual.

In this context, this work has presented a quantitative comparison of the performance of seven different methods for the estimation of the BW present in VOG-SPEM sequences, which is based on the maximum similarity between the estimated BW and a manually delineated GT. In this regard, one of the main contributions of this paper is the proposal of a set of guidelines and a method to manually delineate the GT that was used to isolate the involuntary events considered of interest and for comparison purposes. The development of this protocol has opened the door to propose, for the first time, a set of methods to eliminate the BW from SPEM sequences recorded using VOG means.

For comparison purposes, this work has proposed the use of seven different methods, namely: EMD, VMD, EWT, FDM, EMD2, IIR filtering, and MAF. These methods were objectively evaluated according to four different metrics (PRD, RMSE, MAF, and SNR). The EWT method provided the best performance according to three of the metrics used (PRD, RMSE, and SNR). The results also show that MAF performs well according to the SMAPE metric. In addition, EMD and IIR filtering provide good results, close to those of the EWT. Subjective results also demonstrate that the proposed methods provide very good results, significantly removing all voluntary movements in the VOG-SPEM sequences. This is especially visible when comparing the movements of the left and right eyes. Furthermore, the asymmetries between the movements of both eyes that usually appear due to calibration and recording issues disappeared significantly after removing the BW.

Regardless of the method used to remove the BW from the VOG-SPEM sequences, removing it is considered an essential step to recover the expected synchronisation and symmetries in the movements of both eyes. Besides, this is also considered essential to isolate the involuntary movements and for further automatic processing of them.

Once this step is done, we are in a good position to apply automatic methods to the evaluation and analysis of the residuals, with the aim of characterising the involuntary movements present in the VOG-SPEM sequences using artificial models.

Although this study provided valuable information on the effectiveness of different methods for removing BW from SPEM sequences, several potential limitations exist. First, the sample size for the study was relatively small, with only 52 patients, 60 controls, and 12 young participants. Although this allowed for a detailed comparison of the different BW removal methods, a larger sample size could result in more robust and generalisable findings. Second, the methods used can only be applied to the SPEM analysis. Thus, removing the BW from sequences obtained with other stimuli would require different techniques. This limitation might also apply to SPEM obtained using different amplitudes and/or periods of the target. Third, due to the lack of an existing ground truth, it was manually delineated, which might introduce human bias and subjectivity into the results. Despite these limitations, the results of this study provide valuable insights into the effectiveness of different BW removal methods for SPEM sequences and highlight the importance of removing the BW.

APPENDIX 1

This Appendix contains the results of an ANOVA statistical analysis carried out to check the differences between the metrics calculated to assess the similarity of the GT and the estimated BW for PD patients vs. Ctrl groups, PD patients vs. Yng groups, and Ctrl vs. Yng groups (Table 2). For the comparison between the PD and Ctrl groups, the results show that there are no significant differences between the metrics obtained; but certain differences could exist between the PD and Yng groups, and between the Ctrl and Yng groups, since Yng can follow the target more consistently, likely due to attentional or cognitive matters.

APPENDIX 2

This appendix summarises the results of the experiments performed to select the hyperparameters that provided the best results for each BW removal method used.

For the EMD method, the estimated BW of the VOG-SPEM was calculated by adding the last six IMFs to the residual. This parameter (six) was obtained by iteratively aggregating the IMFs (from last to first) until the best estimate was obtained (Fig. 9a).

For the VMD approach, the IMFs were iteratively aggregated from last to first until the best estimation was obtained.

Fig. 9b reports that only one IMF (the last) is required to get the best performance.

Fig. 9c shows the performance of the FDM method for several cutoff frequencies. Based on the results, the cutoff frequency of the FDM method was selected as 0.6 Hz to provide the best estimate.

The EWT method requires adjusting two hyperparameters: the maximum number of modes and the combination of modes required to estimate the BW.

Fig. 9d shows the performance of BW estimation for this method vs. the maximum number of modes and the combination of modes required. The best performance is obtained using three modes for calculating the EWT, also estimating the BW using three modes.

Fig. 9e compares the performance of the MAF method for different values of k. According to the plot, the best BW estimation was obtained for a value of 600.

The cutoff frequency of the IIR method was experimentally identified by testing different values. According to the results presented in Fig. 9f, it was fixed to 0.5 Hz.

The estimated BW by EMD2 is extracted by summing up the last six IMFs and filtering the residual using a high pass filter with a 0.9 Hz cut-off frequency. This cut-off frequency is obtained experimentally by testing different values according to the results provided in Fig. 9g.

REFERENCES

[1] L. V. Kalia and A. E. Lang, "Parkinson's disease," *Lancet*, vol. 386, no. 9996, pp. 896–912, Aug. 2015.

[2] L. Cipparrone, A. Ginanneschi, F. Degl'Innocenti, P. Porzio, P. Pagnini, and P. Marini, "Electro-oculographic routine examination in Parkinson's disease," *Acta Neurol. Scandinavica*, vol. 77, no. 1, pp. 6–11, Mar. 1988.

[3] M. S. Corin, T. S. Elizan, and M. B. Bender, "Oculomotor function in patients with Parkinson's disease," *J. Neurol. Sci.*, vol. 15, no. 3, pp. 251–265, Mar. 1972.

[4] T. Nakamura, R. Kanayama, R. Sano, M. Ohki, Y. Kimura, M. Aoyagi, and Y. Koike, "Quantitative analysis of ocular movements in Parkinson's disease," *Acta Oto-Laryngol.*, vol. 111, pp. 559–562, Jan. 1991.

[5] R. J. Leigh and D. S. Zee, *The Neurology of Eye Movements*. London, U.K.: Oxford Univ. Press, 2015.

[6] K. Frei, "Abnormalities of smooth pursuit in Parkinson's disease: A systematic review," *Clin. Parkinsonism Rel. Disorders*, vol. 4, Jan. 2021, Art. no. 100085.

[7] S. Stuart, A. Hickey, R. Vitorio, K. Welman, S. Foo, D. Keen, and A. Godfrey, "Eye-tracker algorithms to detect saccades during static and dynamic tasks: A structured review," *Physiol. Meas.*, vol. 40, no. 2, Feb. 2019, Art. no. 02TR01.

[8] V. Lal and D. Truong, "Eye movement abnormalities in movement disorders," *Clin. Parkinsonism Rel. Disorders*, vol. 1, pp. 54–63, Jan. 2019.

[9] H. Zhou, X. Wang, D. Ma, Y. Jiang, F. Li, Y. Sun, J. Chen, W. Sun, E. H. Pinkhardt, B. Landwehrmeyer, A. Ludolph, L. Zhang, G. Zhao, and Z. Wang, "The differential diagnostic value of a battery of oculomotor evaluation in Parkinson's disease and multiple system atrophy," *Brain Behav.*, vol. 11, no. 7, Jul. 2021, Art. no. e02184.

[10] T. J. Anderson and M. R. MacAskill, "Eye movements in patients with neurodegenerative disorders," *Nature Rev. Neurol.*, vol. 9, no. 2, pp. 74–85, Feb. 2013.

[11] E. L. Keller and S. J. Heinen, "Generation of smooth-pursuit eye movements: Neuronal mechanisms and pathways," *Neurosci. Res.*, vol. 11, no. 2, pp. 79–107, Jul. 1991.

[12] C.-C. Wu, B. Cao, V. Dali, C. Gagliardi, O. J. Barthelemy, R. D. Salazar, M. Pomplun, A. Cronin-Golomb, and A. Yazdanbakhsh, "Eye movement control during visual pursuit in Parkinson's disease," *PeerJ*, vol. 6, Aug. 2018, Art. no. e5442.

[13] H. Miyashita, M. Hayashi, and K.-I. Okada, "Implementation of EOG-based gaze estimation in HMD with head-tracker," in *Proc. 18th Int. Conf. Artif. Reality Telexistence*, 2008, pp. 20–27.

[14] T. Haslwanter and A. H. Clarke, "Eye movement measurement: Electro-oculography and video-oculography," in *Handbook of Clinical Neurophysiology*, vol. 9. Elsevier, 2010, pp. 61–79. [Online]. Available: https://www.sciencedirect.com/science/article/abs/pii/S1567423110090052, doi: 10.1016/S1567-4231(10)09005-2.

[15] J. Otero-Millan, S. L. Macknik, and S. Martinez-Conde, "Fixational eye movements and binocular vision," *Frontiers Integrative Neurosci.*, vol. 8, p. 52, Jul. 2014.

[16] A. Spauschus, J. Marsden, D. M. Halliday, J. R. Rosenberg, and P. Brown, "The origin of ocular microtremor in man," *Exp. Brain Res.*, vol. 126, no. 4, pp. 556–562, Jun. 1999.

[17] C. Baek, Y. Goo, and J. M. Seo, "Real-time baseline wander removal from electrooculography using probabilistic baseline prediction," in *Proc. 6th Eur. Conf. Int. Federation Med. Biol. Eng.*, in IFMBE Proceedings, vol. 45, 2015, pp. 78–81.

[18] N. Barbara, T. A. Camilleri, and K. P. Camilleri, "A comparison of EOG baseline drift mitigation techniques," *Biomed. Signal Process. Control*, vol. 57, Mar. 2020, Art. no. 101738.
[19] C. J. De Luca, L. D. Gilmore, M. Kuznetsov, and S. H. Roy, "Filtering the surface EMG signal: Movement artifact and baseline noise contamination," *J. Biomech.*, vol. 43, no. 8, pp. 1573–1579, May 2010.
[20] I. Rodríguez-Carreño, A. Malanda-Trigueros, L. Gila-Useros, J. Navallas-Irujo, and J. Rodríguez-Falces, "Filter design for cancellation of baseline-fluctuation in needle EMG recordings," *Comput. Methods Programs Biomed.*, vol. 81, no. 1, pp. 79–93, Jan. 2006.
[21] L. Sörnmo and P. Laguna, *Bioelectrical Signal Processing in Cardiac and Neurological Applications*. Amsterdam, The Netherlands: Elsevier, 2005.
[22] A. E. Awodeyi, S. R. Alty, and M. Ghavami, "Median based method for baseline wander removal in photoplethysmogram signals," in *Proc. IEEE Int. Conf. Bioinf. Bioeng. (BIBE)*, Nov. 2014, pp. 311–314.
[23] Y. Zhang, B. Liu, and Z. Zhang, "Combining ensemble empirical mode decomposition with spectrum subtraction technique for heart rate monitoring using wrist-type photoplethysmography," *Biomed. Signal Process. Control*, vol. 21, pp. 119–125, Aug. 2015.
[24] J. A. Van Alste and T. S. Schilder, "Removal of base-line wander and power-line interference from the ECG by an efficient FIR filter with a reduced number of taps," *IEEE Trans. Biomed. Eng.*, vol. BME-32, no. 12, pp. 1052–1060, Dec. 1985.
[25] R. P. Narwaria, S. Verma, and P. K. Singhal, "Removal of baseline wander and power line interference from ECG signal–A survey approach," *Int. J. Electron. Eng.*, vol. 3, no. 1, pp. 107–111, 2011.
[26] I. Markovsky, A. Amann, and S. Van Huffel, "Application of filtering methods for removal of resuscitation artifacts from human ECG signals," in *Proc. 30th Annu. Int. Conf. IEEE Eng. Med. Biol. Soc.*, Aug. 2008, pp. 13–16.
[27] J. M. Łęski and N. Henzel, "ECG baseline wander and powerline interference reduction using nonlinear filter bank," *Signal Process.*, vol. 85, no. 4, pp. 781–793, Apr. 2005.
[28] S. Lahmiri and M. Boukadoum, "Physiological signal denoising with variational mode decomposition and weighted reconstruction after DWT thresholding," in *Proc. IEEE Int. Symp. Circuits Syst. (ISCAS)*, May 2015, pp. 806–809.
[29] J. Tang, Q. Zou, Y. Tang, B. Liu, and X.-K. Zhang, "Hilbert–Huang transform for ECG de-noising," in *Proc. 1st Int. Conf. Bioinf. Biomed. Eng. (ICBBE)*, Jul. 2007, pp. 664–667.
[30] S. Lahmiri, "Comparative study of ECG signal denoising by wavelet thresholding in empirical and variational mode decomposition domains," *Healthcare Technol. Lett.*, vol. 1, no. 3, pp. 104–109, Sep. 2014.
[31] S. Lahmiri and M. Boukadoum, "A weighted bio-signal denoising approach using empirical mode decomposition," *Biomed. Eng. Lett.*, vol. 5, no. 2, pp. 131–139, Jul. 2015.
[32] P. B. Patil and M. S. Chavan, "A wavelet based method for denoising of biomedical signal," in *Proc. Int. Conf. Pattern Recognit., Informat. Med. Eng. (PRIME)*, Mar. 2012, pp. 278–283.
[33] B. Weng, M. Blanco-Velasco, and K. E. Barner, "Baseline wander correction in ECG by the empirical mode decomposition," in *Proc. IEEE 32nd Annu. Northeast Bioeng. Conf.*, Apr. 2006, pp. 135–136.
[34] S. L. Joshi, R. A. Vatti, and R. V. Tornekar, "A survey on ECG signal denoising techniques," in *Proc. Int. Conf. Commun. Syst. Netw. Technol.*, 2013, pp. 60–64.
[35] M. S. Chaudhary, R. K. Kapoor, and A. K. Sharma, "Comparison between different wavelet transforms and thresholding techniques for ECG denoising," in *Proc. Int. Conf. Adv. Eng. Technol. Res. (ICAETR)*, Aug. 2014, pp. 1–6.
[36] O. Singh and R. K. Sunkaria, "ECG signal denoising via empirical wavelet transform," *Australas. Phys. Eng. Med.*, vol. 40, no. 1, pp. 219–229, Mar. 2017.
[37] A. Fasano and V. Villani, "Baseline wander removal for bioelectrical signals by quadratic variation reduction," *Signal Process.*, vol. 99, pp. 48–57, Jun. 2014.
[38] B. Lütkenhöner, "Baseline correction of overlapping event-related responses using a linear deconvolution technique," *NeuroImage*, vol. 52, no. 1, pp. 86–96, Aug. 2010.
[39] S. Conforto, T. D'Alessio, and S. Pignatelli, "Optimal rejection of movement artefacts from myoelectric signals by means of a wavelet filtering procedure," *J. Electromyogr. Kinesiol.*, vol. 9, no. 1, pp. 47–57, Jan. 1999.
[40] L. Xu, D. Zhang, K. Wang, N. Li, and X. Wang, "Baseline wander correction in pulse waveforms using wavelet-based cascaded adaptive filter," *Comput. Biol. Med.*, vol. 37, no. 5, pp. 716–731, May 2007.
[41] L. Xu, D. Zhang, and K. Wang, "Wavelet-based cascaded adaptive filter for removing baseline drift in pulse waveforms," *IEEE Trans. Biomed. Eng.*, vol. 52, no. 11, pp. 1973–1975, Nov. 2005.
[42] K. Huda, M. S. Hossain, and M. Ahmad, "Recognition of reading activity from the saccadic samples of electrooculography data," in *Proc. Int. Conf. Electr. Electron. Eng. (ICEEE)*, Nov. 2015, pp. 73–76.
[43] T. Yagi, "Eye-gaze interfaces using electro-oculography (EOG)," in *Proc. Workshop Eye Gaze Intell. Hum. Mach. Interact.*, Feb. 2010, pp. 28–32.
[44] T. Yagi, Y. Kuno, K. Koga, and T. Mukai, "Drifting and blinking compensation in electro-oculography (EOG) eye-gaze interface," in *Proc. IEEE Int. Conf. Syst., Man Cybern.*, Oct. 2006, pp. 3222–3226.
[45] A. Bulling, J. A. Ward, H. Gellersen, and G. Troster, "Eye movement analysis for activity recognition using electrooculography," *IEEE Trans. Pattern Anal. Mach. Intell.*, vol. 33, no. 4, pp. 741–753, Apr. 2011.
[46] M. A. Tinati and B. Mozaffary, "A wavelet packets approach to electrocardiograph baseline drift cancellation," *Int. J. Biomed. Imag.*, vol. 2006, pp. 1–9, Sep. 2006.
[47] M. Mediouni, D. R. Schlatterer, H. Madry, M. Cucchiarini, and B. Rai, "A review of translational medicine. The future paradigm: How can we connect the orthopedic dots better?" *Current Med. Res. Opinion*, vol. 34, no. 7, pp. 1217–1229, Jul. 2018, doi: 10.1080/03007995.2017.1385450.
[48] F. N. Fritsch and R. E. Carlson, "Monotone piecewise cubic interpolation," *SIAM J. Numer. Anal.*, vol. 17, no. 2, pp. 238–246, Apr. 1980.
[49] U. Biswas, M. Maniruzzaman, B. Sana, and K. R. Hasan, "Removing baseline wander from ECG signal using wavelet transform," *Khulna Univ. Stud.*, vol. 16, nos. 1–2, pp. 61–73, 2019.
[50] C.-C. Chen and F. R. Tsui, "Comparing different wavelet transforms on removing electrocardiogram baseline wanders and special trends," *BMC Med. Informat. Decis. Making*, vol. 20, no. S11, pp. 1–10, Dec. 2020.
[51] N. E. Huang, Z. Shen, S. R. Long, M. C. Wu, H. H. Shih, Q. Zheng, N.-C. Yen, C. C. Tung, and H. H. Liu, "The empirical mode decomposition and the Hilbert spectrum for nonlinear and non-stationary time series analysis," *Proc. Roy. Soc. London A, Math., Phys. Eng. Sci.*, vol. 454, no. 1971, pp. 903–995, Mar. 1998.
[52] K. Dragomiretskiy and D. Zosso, "Variational mode decomposition," *IEEE Trans. Signal Process.*, vol. 62, no. 3, pp. 531–544, Feb. 2014.
[53] P. Singh, S. D. Joshi, R. K. Patney, and K. Saha, "The Fourier decomposition method for nonlinear and non-stationary time series analysis," *Proc. Roy. Soc. A, Math., Phys. Eng. Sci.*, vol. 473, no. 2199, Mar. 2017, Art. no. 20160871.
[54] J. Gilles, "Empirical wavelet transform," *IEEE Trans. Signal Process.*, vol. 61, no. 16, pp. 3999–4010, Aug. 2013.
[55] S. Canan, Y. Ozbay, and B. Karlik, "A method for removing low varying frequency trend from ECG signal," in *Proc. 2nd Int. Conf. Biomed. Eng. Days*, 1998, pp. 144–146.
[56] M. Blanco-Velasco, B. Weng, and K. E. Barner, "ECG signal denoising and baseline wander correction based on the empirical mode decomposition," *Comput. Biol. Med.*, vol. 38, no. 1, pp. 1–13, Jan. 2008.
[57] H. Sakoe and S. Chiba, "Dynamic programming algorithm optimization for spoken word recognition," *IEEE Trans. Acoust., Speech, Signal Process.*, vol. ASSP-26, no. 1, pp. 43–49, Feb. 1978.
[58] A. Yazdanbakhsh, C.-C. Wu, B. Cao, V. Dali, C. Gagliardi, M. Pomplun, and A. Cronin-Golomb, "Involuntary saccades and binocular coordination during visual pursuit in Parkinson's disease," *J. Vis.*, vol. 16, no. 12, p. 1358, Aug. 2016.

MEHDI BEJANI received the B.S. degree in electrical engineering from Shahid Rajaee University, Tehran, Iran, in 2007, and the M.Sc. degree in electrical engineering from Islamic Azad University, South Tehran Branch, in 2011. He has been a Researcher with Universidad Politécnica de Madrid (UPM), Spain, since November 2019, and works on the early diagnosis of Parkinson's disease by eye movement using machine-learning techniques. His research interests include eye tracking, EEG, Parkinson's disease, multimodal affective computing, machine learning, and image and speech processing.

ELISA LUQUE-BUZO was born in Madrid, Spain, in 1988. She received the M.D. degree in 2012, and the specialized degree in neurology in 2017. She was trained in movement disorders with the University Hospital Gregorio Marañón. Her research interests include the field of Parkinson's disease and movement disorders.

ARSEN BURLAKA-PETRASH received the B.Sc. degree in biomedical engineering from the Charles III University of Madrid, Spain, in 2019. He is currently a Researcher with Universidad Politécnica de Madrid, Spain. From 2018 to 2019, he was a Research Assistant with the Institute of Polymer Science and Technology, Spanish National Research Council (CSIC), Madrid.

JORGE A. GÓMEZ-GARCÍA received the B.Sc. and M.Sc. degrees from Universidad Nacional de Colombia, Manizales, in 2008 and 2010, respectively, and the Ph.D. degree from Universidad Politécnica de Madrid, Spain, in 2018. He is currently with the Instituto Cajal, Spanish National Research Council (CSIC). His research interests include the use of signal processing and machine learning for biomedical applications, with a focus on the extraction of novel biomarkers for the characterization of neurodegenerative disorders.

JULIÁN D. ARIAS-LONDOÑO (Senior Member, IEEE) received the B.S. degree in electronic engineering and the M.Eng. degree from Universidad Nacional de Colombia, Manizales, Colombia, in 2005 and 2007, respectively, and the dual Ph.D. degree in computer science and automatics from Universidad Politécnica de Madrid (UPM), Spain, and the Universidad Nacional de Colombia, in 2010. Since 2012, he has been with the Department of Systems Engineering and Computer Science, Universidad de Antioquia (UdeA), Medellín, Colombia, where he has been appointed as a Full Professor, since 2020. He is currently a Visiting Researcher with the Department of Signal, Systems and Radiocommunication, ETSIT-UPM, funded by a María Zambrano Grant. He is part of the Intelligence Information Systems Laboratory—UdeA and the Signal Processing Applications Group—UPM. His research interests include the areas of computational intelligence, machine learning, and signal processing applied to biomedical and biological data analysis. Since 2022, he has also been a member of the European Laboratory for Learning and Intelligent Systems (ELLIS) Society.

F. GRANDAS-PÉREZ is currently pursuing the M.D. degree in neurology with the University Hospital of Oviedo, Spain. He was trained in movement disorders at the Maudsley Hospital, London, U.K. He has been a Professor of neurology with the Universidad Complutense, Madrid, Spain, since 2017, and the Head of the Department of Neurology of the University Hospital Gregorio Marañón, Madrid, since 2014. His research interests include the field of Parkinson's disease and movement disorders.

JESUS GRAJAL (Senior Member, IEEE) was born in Toral de los Guzmanes, Leon, Spain, in 1967. He received the degree in telecommunications engineering and the Ph.D. degree from Universidad Politécnica de Madrid, Madrid, Spain, in 1992 and 1998, respectively. Since 2017, he has been a Full Professor with the Signals, Systems, and Radio Communications Department, Universidad Politécnica de Madrid. His research interests include semiconductor device modeling and high-frequency circuit and system design. He was a corecipient of the 2013 EuCAP Best Antenna Design Paper Award.

JUAN IGNACIO GODINO-LLORENTE (Senior Member, IEEE) was born in Madrid, Spain, in 1969. He received the B.Sc. and M.Sc. degrees in telecommunications engineering and the Ph.D. degree in computer science from Universidad Politécnica de Madrid (UPM), Spain, in 1992, 1996, and 2002, respectively. From 1996 to 2003, he was an Assistant Professor with the Circuits and Systems Engineering Department, UPM. From 2003 to 2005, he joined the Signal Theory and Communications Department, University of Alcalá. In 2005, he joined UPM again, being the Head of the Circuits and Systems Engineering Department, from 2006 to 2010. Since 2011, he has been a Full Professor with the Signal Systems and Radio Communications Department, UPM. He has also been the Spanish Coordinator of the 2103 COST Action funded by the European Science Foundation and the General Chairperson of the Third Advanced Voice Function Assessment Workshop. During his career, he has led more than 20 research projects funded by national and international public bodies and industries. From 2003 to 2004, he was a Visiting Professor with Salford University, Manchester, U.K. In 2016, he was a Visiting Researcher with the Massachusetts Institute of Technology, Cambridge, MA, USA, funded by a Fulbright Grant. He has served as an Editor for *Speech Communication*, the *EURASIP Journal on Advances in Signal Processing*, the IEEE JOURNAL OF SELECTED TOPICS IN SIGNAL PROCESSING (JSTSP), and the IEEE TRANSACTIONS ON AUDIO, SPEECH, AND LANGUAGE PROCESSING (TASLP).